ISIJ International, Vol. 51 (2011), No. 5, pp. 769–775

On the Representativeness of Automated SEM/EDS Analyses for Inclusion Characterisation with Special Regard to the Measured Sample Area

Susanne K. MICHELIC, Gerhard WIESER and Christian BERNHARD

Montanuniversitaet Leoben, Franz-Josef-Straße 18, 8700 Leoben, Austria.
E-mail: susanne.michelic@unileoben.ac.at, gerhard.wieser@unileoben.ac.at, christian.bernhard@unileoben.ac.at

(*Received on December 6, 2010; accepted on January 28, 2011*)

The cleanness of steel has emerged to an important quality criterion for a wide field of special applications. In order to ensure the reliable characterisation of non-metallic inclusions, the constant optimisation of current analysing methods is essential. The present study focuses on the automated SEM/EDS analysis, especially determining the influence of the analysed sample area on the obtained particle diameters and size distributions of non-metallic inclusions. Besides the experimental analysis of different area sizes, a model was formulated to estimate the error of area ratio as a function of inclusion content. For the assumed conditions, an area range combining a sufficient and significant area size with a feasible time effort is defined. The model also evaluates the significance of the results for the maximum and medium particle diameter gained out of the measurements. Moreover, the truncation of the data – resulting from an experimental analysing limit – and its consequences are discussed. The results underline the potential of this analysing method for inclusion characterisation but also demonstrate the limitations especially regarding the maximum particle diameter. This work contributes to a better understanding in terms of representativeness of automated SEM/EDS analysis and provides important information for further practical analyses.

KEY WORDS: non-metallic inclusion; automated SEM/EDS analysis; sample area; particle diameter; truncation.

1. Introduction

The production of metallic alloys via the liquid phase often results in the formation of non-metallic inclusions (NMIs). These are mostly undesired and can substantially decrease the final product quality. Depending on the field of application, each alloy has different requirements on morphology, amount and distribution as well as chemistry of NMIs. In order to verify and improve the steel cleanness continuously, a reliable characterisation of non-metallic inclusions is indispensable. In **Fig. 1** some of the current analysing methods for the characterisation of NMIs are summarised and compared. A general assessment of these methods is rather difficult, owing to the large amount of appraisal factors: Next to the information content of the results (chemical and/or morphological data), the detectable range of inclusion sizes as well as the analysed sample volume – respectively area – are fundamental points of interest. Although the more information can be gained the better, the complexity of analysis must be considered in practice.

In spite of the considerable effort related to automated SEM/EDS analyses, this method has become state of the art[11–13] not only in the field of material characterisation but also concerning metallurgical process control and optimisation. However, the automated SEM/EDS analysis is based on a two-dimensional view of inclusions distributed in space. Even if this reduction of dimensions brings along a substantial facilitation for the measuring process – considering the fact that a particle is not cut at its maximum diameter necessarily – a metallographic specimen yields only an apparent distribution of the inclusion diameters (see **Fig. 2**).

Thus, two decisive questions for two-dimensional inclusion analysis arise: Firstly, whether the sample area is sufficient to determine large, however stochastically rare inclusions. Secondly, if the analysis of a defined sample area is adequate to give an impression of the global cleanness (also involving the influence of smaller inclusions) of a whole volume. The first question has extensively been treated in the last years by different theoretical approaches.[15–31] The second question of general representativeness of a defined sample area has not been addressed precisely so far. The present work focuses on the characterisation of NMIs using automated SEM/EDS analyses. Due to the combination of low occurrence of inclusions in clean steels and the practically limited testing volumes of most cleanness assessment methods, the significance of the results strongly depends on the size of the analysed area. In order to answer the question of the representative sample area and its impact on the inclusion size distribution, within this study experimental mea-

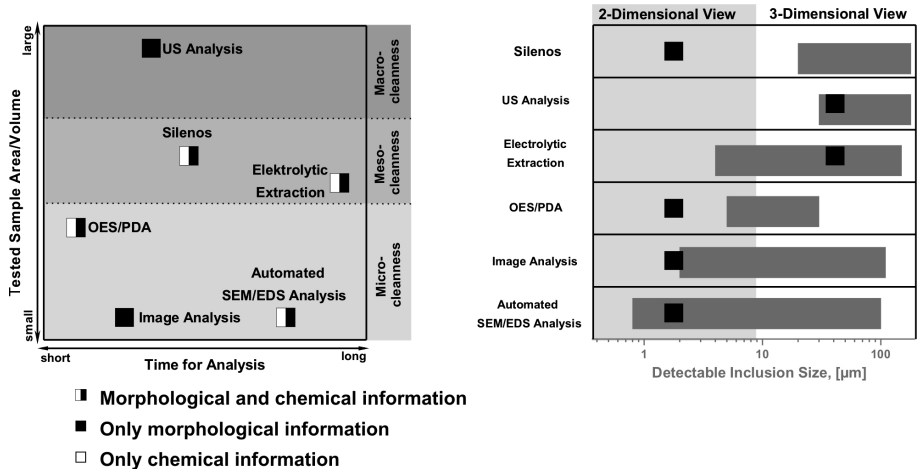

Fig. 1. Comparison of some current methods for inclusion characterisation.[1–10)]

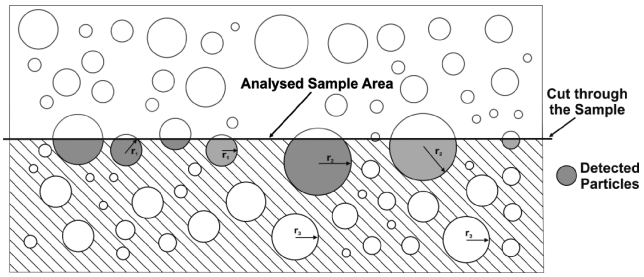

Fig. 2. Scheme of an apparent size distribution of non-metallic inclusions on a metallographic specimen, according to[14)].

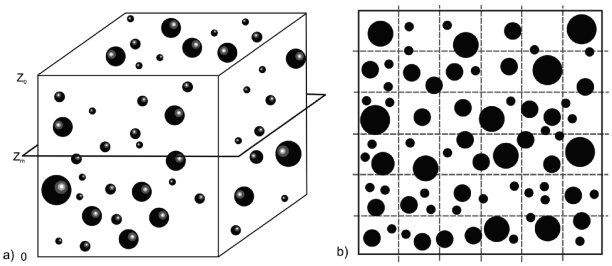

Fig. 3. a) Schematic illustration of a cube with distributed spheres. b) Schematic cut through the cube plane parallel to the cube base.

surements are coupled with a statistical - geometric model of the problem.

2. Model Formulation

For inclusion characterisation using the SEM/EDS method, a planar metallographic specimen is necessary. In order to describe the representative sample area in dependence of sample volume and inclusion content, the following model was formulated: A defined number of inclusions was distributed in a cube. Although NMIs can show very complex geometries in reality, the model is currently based on the assumption of spherical shapes only. As illustrated in **Fig. 3**(a), the individual spheres with the centre coordinates $S_i=(s_{x,i},s_{y,i},s_{z,i})$ are randomly distributed in the cube, with the diameters of the spheres d_i according to a lognormal distribution $\aleph(\mu,\sigma)$.
Thus,

$$\frac{1}{\sqrt{2\pi}\sigma}\sum_{0}^{N_D}\frac{1}{d_i}\exp\left(-\frac{\ln(d_i-\mu)}{2\sigma^2}\right)\cong 1 \quad \text{..... (1)}$$

where μ, σ are the mean and the standard deviation of the applied lognormal distribution, respectively; N_D is the amount of distributed spheres per mm^3. Upon initialisation, the positions of the spheres are arbitrarily determined. The required input parameters, i.e., N_D, μ and σ are chosen according to the experimental results (see subsequent section). Since these parameters depend on the inclusion content N_A on the sample area, they are varying for every steel grade.

Hence, the cube is numerically intersected m times with the intersection plane parallel to the cube base. The position of the plane is termed z_m with $0<z_m<z_0$ where $x_0=y_0=z_0$ is the cube side length. The set of spheres $\overline{S}_m$ cut by the plane m, schematically illustrated in Fig. 3(b), is determined by

$$\overline{S}_m=\left\{s_{z,i}-d_i/2\le z_m\le s_{z,i}+d_i/2;0<i\le N_D\right\} \quad \text{..... (2)}$$

Since the spheres of each set $\overline{S}_m$ are actually cut at different distances from their centre points, the diameters of the resulting intersections (circles) need to be determined individually. Evidently, their calculation results from

$$d_{i,m}^c=2\sqrt{\left(\frac{d_i}{2}\right)^2-\left|z_m-s_{z,i}\right|^2} \quad \text{..... (3)}$$

where $d_{i,m}^c$ are the diameters of the respective intersection circles. Hence, the total area of all intersected circles $\overline{A}$ is given by

$$\overline{A}=\frac{\pi}{4}\sum_m\sum_i(d_{i,m}^c)^2 \quad \text{..... (4)}$$

In the present model $m=5$, therefore the maximum virtual analysed sample area is 2 000 mm² since each intersection plane has an area of 400 mm². Evidently the maximum sample area thus exceeds virtually any practically employed experimental analysing area (typically<400 mm²). Thus, the high ratio between analysed sample area and total sample volume ensures an unbiased, stochastic distribution of the particles.

By numerically limiting the single intersection place, the influence of the minimisation of analysed sample area could be studied. The error in analysed sample area is

finally given by

$$Error = \frac{\overline{A} - A_T}{A_T} 100\% \quad \text{..... (5)}$$

where A_T is the area of all intersected circles at the maximum intersection area of 2 000 mm².

Moreover, in difference to the results of the automated SEM/EDS analyses, there is no truncation limit for the circle diameter in the model. Hence, the sum of all intersected spheres equals entirety. In order to analyse the influence of this truncation, the truncation limit from the practical observations (1.1 μm) is also introduced numerically. Given that the diameters in $d_{i,m}^{c}$ follow the lognormal distribution $\aleph(\tilde{\mu},\tilde{\sigma})$, the distribution parameters could further be obtained.

3. Experimental Procedure

By using the automated SEM/EDS analysis for the characterisation of cleanness in steels, NMIs are detected due to material contrast differences in the backscattered electron (BSE) image. The output consists of the position and the morphological data of every detected particle as well as its chemical composition. The latter is only listed for reasons of completeness, the present work primarily deals with the morphological properties of inclusions. In general, all inclusion types can be detected simultaneously during the measurement. This study concentrates on Al_2O_3 inclusions – only this inclusion type is evaluated in the practical part. Consequently, the theoretical results are also only valid for the defined inclusion content. When interpreting the results, also the truncation of data must be considered: For every analysis, the minimum number of pixels which is needed to identify a particle has to be defined. In the present study a resolution of 1 024 px × 960 px is used. In order to be detected as a particle, at least 4 connected pixels have to show a greyscale value different to the matrix. Depending on the magnification and the resolution, the area of each included particle is measured; out of it, the so-called Equivalent Circle Diameter (ECD) is calculated,

$$ECD = \sqrt{\frac{4A}{\pi}} \quad \text{..... (6)}$$

For the used SEM/EDS device, the practical limit lies at an ECD of 0.6 μm. Usually, a limit of 1.1 μm is used, achieving an acceptable compromise between measuring time and obtained results. Consequently not the whole size spectrum of NMIs is analysed. Furthermore, the determination of the ECD can be difficult for several fine agglomerated inclusions, appearing as one large particle for the system and hence presenting an inaccurate ECD. In the case of the used settings, two particles are detected separately, if at least two connected pixels between them have a grey scale value different to the defined threshold. In order to avoid such incorrect measurements, a subsequent manual verification of the results is advisable. The settings applied for the automated SEM/EDS analysis are summarised in **Table 1**.

For all measurements a stainless steel sample was used. The steel was melted in an induction furnace at the Chair of Metallurgy; its composition is shown in **Table 2**. Out of the cast steel ingot a cuboid with the dimensions 49×49×65 mm³ was formed at 1 200°C with a deformation degree of φ=0.7. The subsequent metallographic sample preparation was also performed at the Chair of Metallurgy. In order to study the influence of the measurement area, three different sizes of sample areas were analysed. For this purpose an area of 50 mm² was enlarged continuously (see **Fig. 4**), always using the identical SEM/EDS settings and a minimum feature diameter of 1.1 μm. When superimposing the three iterations for the results of 50 mm², an accordance of 99% is observed. Consequently, variations resulting out of measurement influences are negligible.

Table 1. Experimental settings.

Beam energy	15 keV
Working distance	10 mm
Resolution	1 024 px × 960 px
Magnification	600x
Minimum particle size	4 px
EDS evaluation time for one particle	3 s

Table 2. Chemical composition of the steel used in the experimental part in wt.-%.

%C	%Cr	%Si	%Mn	%Mo	%V
0.34	5.02	1.57	0.53	1.28	0.49

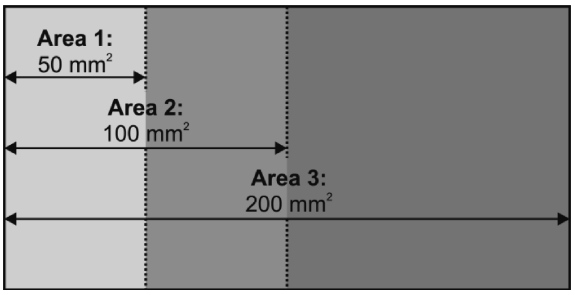

Fig. 4. Schematic illustration of the arrangement of the different used measuring areas.

4. Results

4.1. Experimental Variation of Analysed Sample Area

4.1.1. Distribution of NMI on the Analysed Sample Area

Figure 5 shows the positions of detected Al_2O_3 inclusions on the measured sample area of 200 mm². The inclusions are scaled in four size classes ranging between 1 and 20 μm ECD. In the present case, the particles are distributed very homogenously and the majority of inclusions is smaller than 10 μm.

Two examples of SEM-images of Al_2O_3 inclusions detected on the measured sample area are displayed in **Fig. 6**. Both particles show a very globular shape, whereat one is significantly smaller than the other. Looking at the corresponding EDS analyses in **Fig. 7**, the effect of particle size on the measured spectrum for the used settings can be seen. Dependent on the chosen accelerating voltage a certain sample volume gets activated and the detected elements are

displayed in the resulting EDS spectrum. In general, the larger the particle, the smaller is the amount of measured matrix around the inclusion. While due to an ECD of the particle < 2 μm in the case of spectrum 1 several matrix elements are detected, spectrum 2 only shows the elements the measured inclusion is composed of. This effect always has to be considered when dealing with the chemical composition of non-metallic inclusions.

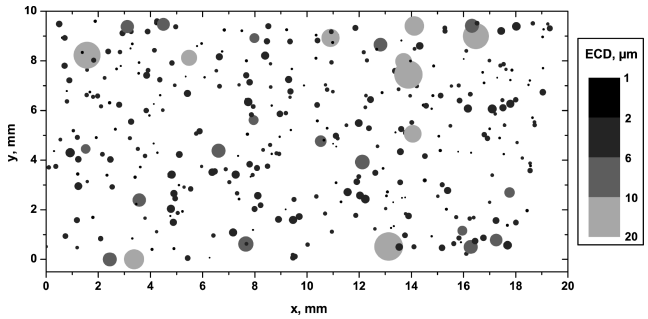

Fig. 5. Illustration of the distribution of detected Al_2O_3 inclusions on a measured sample area of 200 mm^2 scaled in different size classes.

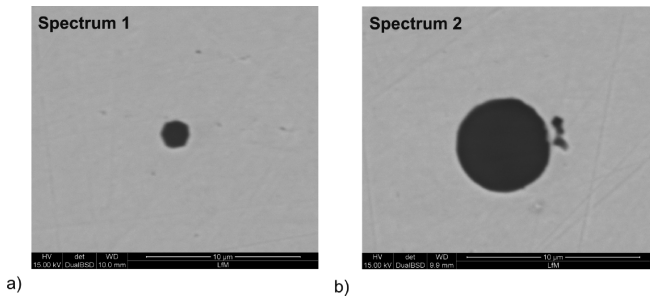

Fig. 6. Exemplary SEM-images of detected Al_2O_3 particles on the analysed sample area.

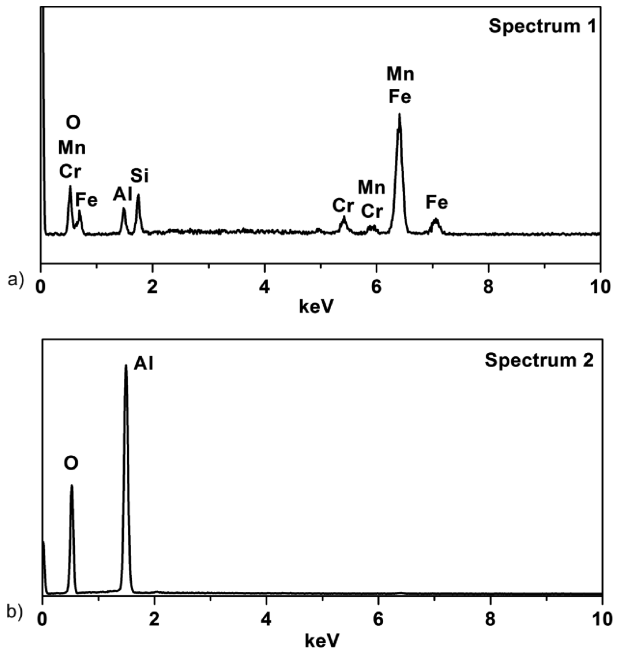

Fig. 7. Corresponding EDS analyses to Al_2O_3 particles shown in Fig. 6.

4.1.2. Medium and Maximum Particle Diameter

Figure 8(a) demonstrates the percentage of NMIs with an ECD < 5 μm as a function of the measured area. In all cases more than 87% of all Al_2O_3 particles have an ECD < 5 μm; the medium ECD amounts to app. 3 μm for all analysed areas. Although slight variations are found in the results for the maximum ECD (see Fig. 8(b)) there is no significant increase of the maximum detected inclusion size with larger measuring area; no outlier can be observed. Theoretically it is also imaginable that in spite of increasing the measuring area, the largest inclusion is detected in the smallest analysing field. Therefore, locating a larger particle is not only difficult even on a larger analysing area, but foremost varies considerably.

4.1.3. Size Distributions

Figure 9 illustrates a typical output of automated SEM/EDS analysis. Evidently, the overall number of detected particles increases with larger measuring area. The overall inclusion content amounts to app. 2 Al_2O_3 per mm^2 in all three cases and the maximum lies in the class between 1 and 2 μm ECD. Out of this illustration no considerable disparities can be found. **Table 3** summarises the results for μ_A, σ_A and the inclusion content N_A for the three different measured area sizes. A reasonable consistency is achieved for these values. Anyhow, neither the size distribution nor the values in Table 3 give a concrete conclusion regarding the maximum particle diameter.

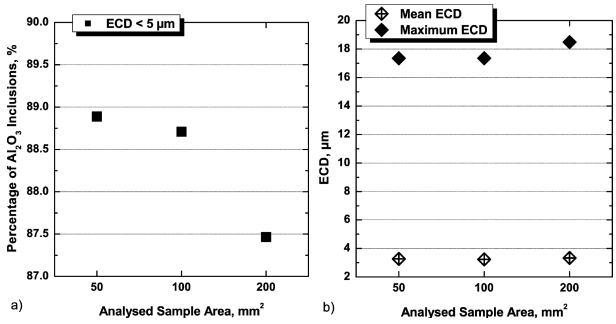

Fig. 8. a) Percentage of NMIs with an ECD < 5 μm as a function of the analysed sample area.b) Experimental results concerning the mean and maximum ECD for different sample areas.

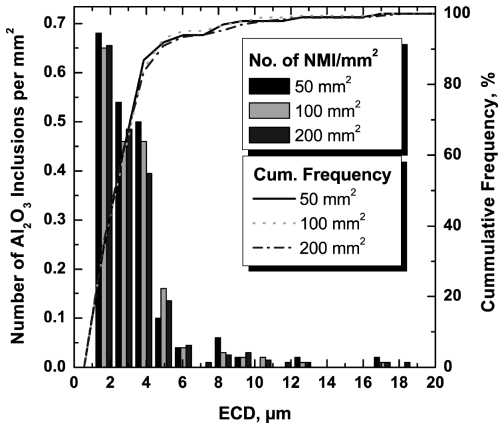

Fig. 9. Number of Al_2O_3 inclusions per mm^2 between 1 and 20 μm ECD on the different analysed area sizes.

Table 3. Values of μ and σ and the inclusion content for different measured area sizes.

	Truncation Limit 1.1 μm		
Area, mm²	μ_A, μm	σ_A, μm	N_A, mm^{-2}
50	3.27	2.38	1.98
100	3.23	2.13	1.86
200	3.33	2.45	1.83

Table 4. Constant simulation parameters.

Cube Side Length	20 mm
N_D	1 217 mm^{-3}
μ	1.88 μm
σ	1.69 μm

With the aid of the practical results from the measurements of 200 mm^2, the input parameters for the statistical - geometric model were defined. Therefore, in a first step, it was necessary to estimate values for the medium sphere diameter μ, standard deviation σ and the number of distributed spheres per volume unit, N_D. For this purpose the following approach was employed, where η_{dA} is the harmonic mean of all measured particle diameters on the area 200 mm^2:[32]

$$\mu = \frac{\pi}{2} \cdot \eta_{dA} \quad \text{..... (7)}$$

$$\sigma = \frac{1}{2}\sqrt{\eta_{dA} \cdot \left|8\mu_A - \pi^2 \eta_{dA}\right|} \quad \text{..... (8)}$$

$$N_D = \frac{2}{\pi}\frac{N_A}{\eta_{dA}} \quad \text{..... (9)}$$

Although a useful estimation basis, the values gained by this approach are not definite, owing to the fact that they are based on truncated data. Therefore, in a subsequent optimisation step, the final input parameters for the statistical - geometric model were gained by iterations over N_D, μ and σ until convergence with the experimental results was achieved; the results of this additional iteration can be found in **Table 4**. The maximum sphere diameter distributed in the cube was defined with 110 μm.

4.2. Results of the Model

4.2.1. Representative Sample Area as a Function of the Inclusion Content

Table 5 summarises the results for $\tilde{\mu}$ and $\tilde{\sigma}$ of the circles as well as the inclusion content $\tilde{N}_A$, for the two different truncation limits for 10 intersections, each with an area of 200 mm^2. It is obvious that the number of inclusions per mm^2 increases with decreasing truncation limit. Evidently, $\tilde{\mu}$ is smaller for 0 μm than 1.1 μm, against what $\tilde{\sigma}$ is smallest for a truncation limit of 1.1 μm. In difference to the results of the automated SEM/EDS analyses, there is no bottom limit for the circle diameter in the calculations. The mean value and the standard deviation of the error of the area ratio of the NMIs are displayed in dependence of the measuring area in **Fig. 10**. The indicated error is displayed with a negative algebraic sign; since in practice usually a lower number of particles – resulting in a smaller area ratio – is detected during the measurement.

Table 5. Values of $\tilde{\mu}$ and $\tilde{\sigma}$ and the inclusion content for different truncation limits.

	Truncation Limit 0.0 μm			Truncation Limit 1.1 μm		
Section	$\tilde{\mu}$, μm	$\tilde{\sigma}$, μm	$\tilde{N}_A$, mm^{-2}	$\tilde{\mu}$, μm	$\tilde{\sigma}$, μm	$\tilde{N}_A$, mm^{-2}
1	2.76	2.75	2.36	3.52	2.86	1.73
2	2.61	2.38	2.34	3.33	2.41	1.71
3	2.55	2.65	2.34	3.38	2.79	1.63
4	2.80	2.90	2.44	3.42	3.02	1.89
5	2.72	2.62	2.26	3.52	2.68	1.62
6	2.84	5.20	2.30	3.46	5.76	1.79
7	2.67	2.89	2.19	3.34	3.06	1.64
8	2.75	2.46	2.26	3.43	2.49	1.70
9	2.62	2.67	2.37	3.31	2.80	1.75
10	2.56	2.54	2.42	3.35	2.66	1.70

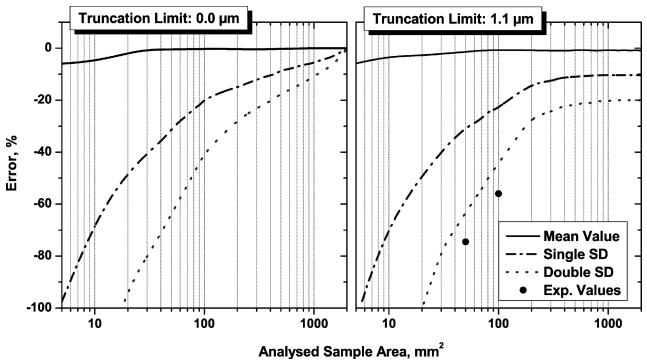

Fig. 10. Error of area ratio in dependence of the analysed sample area for different truncation limits (SD: Standard Deviation).

The values of the error of area ratio resulting from the experimental data are also displayed for the truncation limit of 1.1 μm. In contrast to calculations where the reference area is 2 000 mm^2, the evaluation basis for the experimentally determined values was 200 mm^2, due to the mentioned practical limitations. Therefore, it is comprehensible that these are found outside of the calculated range. Nonetheless comparative results could be obtained. In case of the truncation of 0.0 μm, no sensible experimental points can be plotted in the diagram.

Out of the results in Fig. 10 the following conclusions can be drawn for the application of automated SEM/EDS analyses for the defined conditions:

- If an area of 200 mm^2 – a defined number of inclusions per mm^2 provided – is measured by presetting a minimum particle diameter of 1.1 μm, the mean error of the measured area ratio lies approximately at 2%. Looking at the standard deviation, in the worst case the error can amount to nearly 30%. It must be noticed that in this case relatively low inclusion content was assumed, since all the practical examinations were done for a single inclusion type in the steel matrix.
- Pertaining to the data truncated at 1.1 μm, it can be concluded that an increase of the analysed sample area

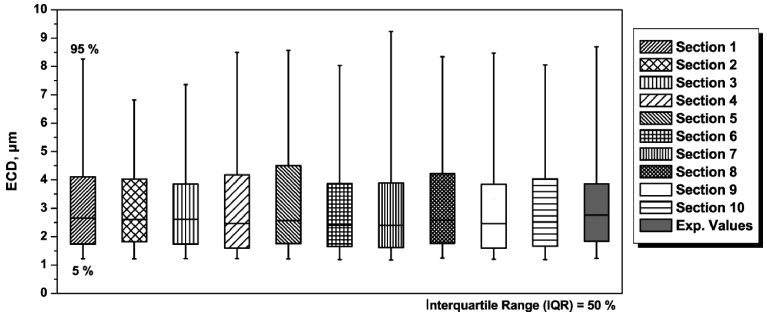

Fig. 12. Box Plot of particles for the 10 sections of the calculations compared to the measured values of Al_2O_3 resulting from the analysis of 200 mm^2.

above 200 mm² would not effectively ameliorate the results, as there is no noticeable influence on the resulting error due to the truncation of the data. A comparison between the two truncation limits in Fig. 10 shows that the truncation of the experimental data implies a certain systematic error, independent of the analysed area.

- In contrast to this, a reduction of the measured area causes a rapid and significant increase of the error. An area of 100–200 mm^2 seems to be a reasonable compromise under the given parameters.
- Regarding the only theoretical possibility that particles of all size classes could be detected, it is shown that the error is clearly smaller. In this case however, a reduction in analysed area will inevitably lead to a remarkably broader scattering of the values, indicated by the increasing standard deviation.

4.2.2. Comparison between Size Distributions of Calculated and Measured Particles

Figure 11 shows the size distributions between 0 and 9.9 μm ECD for the ten sections of the calculations compared to the measured values resulting from the analysis of 200 mm^2. Considering that this is a comparison of absolute values, the results show a good comparability. The variation between the single calculated planes indicates the effect of the probability of intersection mentioned in the introduction. In **Fig. 12** the results of calculated and experimental outputs are compared in a Box-Whisker-Plot. It can be noticed that the interquartile ranges yield approximately equivalent results. Regarding the range in between of which 90% of the values are located, a higher scattering is observed. However, extreme outliers cannot be found.

4.2.3. Comparison between Maximum and Medium Diameter of Calculated and Measured Particles

An overview on the medium and maximum particle diameters for the 10 sections in comparison to the measured results is given in **Fig. 13**. In this case, large variations are obtained primarily concerning the maximum ECD. The largest distributed particle in the model had an ECD of 110 μm. In one section, the maximum diameter is 102 μm, against what the majority – also the experimental value – lies in a range between 20 and 30 μm ECD. This reflects the randomness regarding the maximum ECD of particles – also a very large measuring area is not a warranty for the detecting the largest particle for the reasons mentioned beforehand.

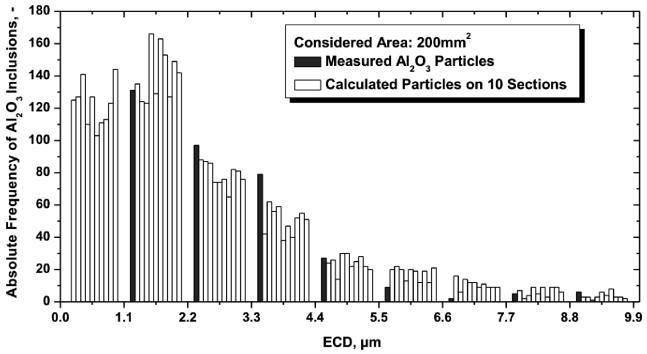

Fig. 11. Size distribution of particles for the 10 sections of the calculations compared to the measured values of Al_2O_3 resulting from the analysis of 200 mm^2.

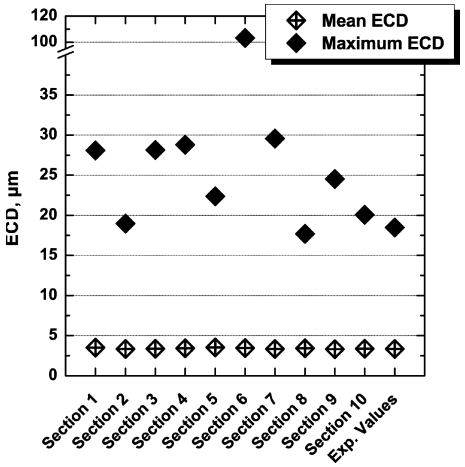

Fig. 13. Medium and maximum particle diameters for the 10 sections of the calculations compared to the measured values of Al_2O_3 resulting from the analysis of 200 mm^2.

5. Summary and Conclusions

One of the most frequently applied methods for cleanness measurements of steels is the automated SEM/EDS analysis. The present study deals with the representativeness of this method with special regard to the measured sample area. In the experimental part, different sizes of sample areas were investigated focussing on the size distributions of the non-metallic inclusions as well as the medium and the maximum diameter of the particles. Based on the experimental investigations a statistical - geometric model was formulated giving the chance of getting an impression of the whole size

distribution. A practical analysing limit inflicts a lower bound for experimental measurements, which therefore always yields truncated data. In dependence of the analysed area and the inclusion content, it is possible to calculate the error of the area ratio.

It could be concluded that the analysis of an area of 100–200 mm^2 offers a valuable basis for the analysis under the assumed conditions. Because of the truncation of data, a significant increase of analysing area, also resulting in a considerable increase of measuring time, would not result in a more representative output in this case. On the contrary, only a slightly smaller measuring area provokes a substantial increase of the error and is therefore not recommended in order to get a meaningful impression on the inclusion landscape. Regarding the maximum inclusion diameter, it has been shown that substantial differences are observed for various calculated and experimental sections. While the maximum sphere diameter distributed in space was defined with 110 μm, only in one calculated section, a circle diameter > 100 μm was found. Consequently, the significance of automated SEM/EDS analysis regarding the maximum diameter in a defined sample volume is very limited. By the presented model, a quantification of the error that is made for defined analysing conditions is available. Thus, conclusions on the representative sample area for steels with a comparable size distribution and inclusion content can be made and very useful information for further practical analyses is achieved. A significant change of inclusion content or the parameters μ and σ will influence the results substantially. In order to upgrade the model and to provide data for different levels of steel cleanness, calculations with different input parameters are planned.

Acknowledgments

This research activity was partly achieved within the Competence Center for Excellent Technologies in "Advanced Metallurgical and Environmental Process Development – K1-MET". The authors would like to thank all members of the "Cleanness Research Group" at the Chair of Metallurgy for the fruitful discussions.

REFERENCES

1) L. Zhang and B. G. Thomas: *ISIJ Int.*, **43** (2003), 271.
2) L. Zhang and B. G. Thomas: *Metall. Mater. Trans. B*, **37B** (2006), 733.
3) M. D. Jaraković, L. B. Nedeljković and M. B. Durdević: *Prakt. Metall.*, **33** (1996), 281.
4) H. V. Atkinson and G. Shi: *Prog. in Mater. Sci.*, **48** (2003), 457.
5) R. Meilland and L. Dosdat: *Rev. Métall.*, **99** (2002), 373.
6) M. Göransson and P. G. Jönsson: *ISIJ Int.*, **41** (2001), S42.
7) R. Meilland, H. Hocquaux, C.Louis, L. Pollino and F. Hoffert: *Rev. Métall.*, **96** (1999), 90.
8) F. Reinholdsson, A. Lind, R. Nilsson, P. Sjödin and P. Jönsson : *ISIJ Int.*, **37** (1997), 637.
9) H. Eichelkraut and M. Weinberg: XXIX. Verformungskundliches Kolloquium, Planneralm, (2010).
10) M. Nuspl, W. Wegscheider, J. Angeli, W. Posch and M. Mayr: *Anal. Bioanal. Chem.*, **379** (2004), 640.
11) S.-R. Story, G.-E. Goldsmith and G.-L. Klepzig: *Rev. Métall.*, **105** (2008), 272.
12) G. Gigacher, W. Krieger, P. R. Scheller and C. Thomser: *Steel Res.*, **76** (2005), 644.
13) W. Winkler, J. Angeli and M. Mayr: *BHM*, **152** (2007), 4.
14) M. Pohl, M. Merz and W.-G. Burchard: Berichte der VI. Int. Metallographie-Tagung, Leoben, (1982), 126.
15) Y. Murakami, Y. Uemura and K. Kawakami: *J. Jpn. Soc. Mech. Eng.*, **1** (1989), 58.
16) Y. Uemura and Y. Murakami: *J. Jpn. Soc. Mech. Eng.*, **1** (1990), 162.
17) Y. Murakami, T. Toriyama and E. M. Coudert: *JTEVA*, **22** (1994), 318.
18) Y. Murakami: *J. Res. Natl. Inst. Stand. Technol.*, **99** (1994), 345.
19) T. Toriyama, Y. Murakami, T. Yamashita, K. Tsubota and K. Furumura: *Tetsu-to-Hagané*, **81** (1995), 77.
20) Y. Murakami, M. Takada and T. Toriyama: *Int. J. Fatigue*, **16** (1998), 661.
21) S. Zhou, Y. Murakami, Y. Fukushima and S. Beretta: *Tetsu-to-Hagané*, **87** (2001), 22.
22) G. Shi, H. V. Atkinson, C. M. Sellars and C. W. Anderson: *Ironmaking Steelmaking*, **26** (1999), 239.
23) G. Shi, H. V. Atkinson, C. M. Sellars and C. W. Anderson: *Acta Mater.*, **47** (1999), 1455.
24) G. Shi, H. V. Atkinson, C. M. Sellars and C. W. Anderson*: Ironmaking Steelmaking*, **27** (2000), 355.
25) G. Shi, H. V. Atkinson, C. M. Sellars and C. W. Anderson: *Ironmaking Steelmaking*, **27** (2000), 361.
26) C. W. Anderson, G. Shi, H. V. Atkinson and C. M. Sellars: *Acta Mater.*, **48** (2000), 4235.
27) H. V. Atkinson, G. Shi, C. M. Sellars and C. W. Atkinson: *Mater. Sci. Technol.*, **16** (2000), 1175.
28) G. Shi, H.V. Atkinson, C. M. Sellars, C. W. Anderson and Y. R. Yates: *Acta Mater.*, **49** (2001), 1813.
29) S. Beretta and Y. Murakami: *Metall. Mater. Trans. B*, **32** (2001), 517.
30) S. Beretta, C. Anderson and Y. Murakami: *Acta Mater.*, **54** (2006), 2277.
31) C. W. Anderson, G. Shi, H. V. Atkinson, C. M. Sellars and J. R. Yates: *Acta Mater.*, **51** (2003), 2331.
32) J. Takahashi and H. Suito: *Mater. Sci. Technol.*, **18** (2002), 103.